NANO LETTERS

Letter

pubs.acs.org/NanoLett

Significantly Improved Trapping Lifetime of Nanoparticles in an Optical Trap using Feedback Control

Arvind Balijepalli,*[,†] Jason J. Gorman,[‡] Satyandra K. Gupta,[§] and Thomas W. LeBrun*[,†]

[†]Physical Measurement Laboratory and [‡]Engineering Laboratory, National Institute of Standards and Technology, Gaithersburg, Maryland 20899, United States

[§]Department of Mechanical Engineering, University of Maryland, College Park, Maryland 20742, United States

ABSTRACT: We demonstrate an increase in trapping lifetime for optically trapped nanoparticles by more than an order of magnitude using feedback control, with no corresponding increase in beam power. Langevin dynamics simulations were used to design the control law, and this technique was then demonstrated experimentally using 100 nm gold particles and 350 nm silica particles. No particle escapes were detected with the controller on, leading to lower limits on the increase in lifetime for 100 nm gold particles of 26 times (at constant average beam power) and 22 times for 350 nm silica particles (with average beam power reduced by one-third). The approach described here can be combined with other techniques, such as counter propagating beams or higher-order optical modes, to trap the smallest nanoparticles and can be used to reduce optical heating of particles that are susceptible to photodamage, such as biological systems.

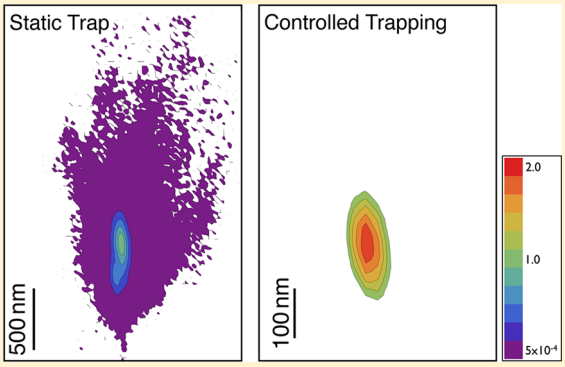

KEYWORDS: *Optical trapping, feedback control, trap lifetime, nanomanipulation, FPGA*

The manipulation and assembly of microscale particles in fluids using optical tweezers are widely used in many areas of research. However, the extension of optical trapping to nanoscale assembly remains undeveloped due to a need for enhanced trapping performance for small nanoparticles. Specifically, there is a need to increase trapping lifetime, reduce optical heating, and increase localization. Here we address the first two objectives and demonstrate enhanced trapping using control systems which are able to confine nanoparticles to an optical trap when a static trap, at the same average beam power, is not able to. Furthermore, these techniques significantly reduce the average power required to trap a particle. Therefore, we believe damage to particles in the trap can be mitigated, which can be particularly beneficial when trapping nanoscale biological particles. Moreover, the development of enhanced nanoparticle trapping may lead to more effective nanomanipulation techniques and to the development of controlled optical trapping as a flexible tool for prototyping and testing novel three-dimensional (3D) nanodevices.

A significant challenge to confining nanoparticles to a trap is that for a constant beam power, the optical forces acting on a nanoparticle decrease significantly as a function of its size. Moreover, simply increasing the power of the incident beam to increase the force acting on the particle is also problematic. Recent work has demonstrated that even when using laser powers as high as 855 mW (which can result in power densities of hundreds of megawatts per square centimeter for diffraction limited traps), gold nanoparticles with a diameter of 18 nm, dispersed in water, were only confined to an optical trap for a few seconds at a time, which limits their utility in nanoassembly applications.[1] Furthermore, particles smaller than 18 nm could not be localized when using even higher laser powers. An additional detrimental effect of using high laser powers is the significant heating of nanoparticles that may cause them irreversible damage. Seol et al. have studied the effect of particle-mediated heating (calculated at the peak intensity of the beam) for 100 nm gold nanoparticles due to absorption and found significant heating of up to 266 °C/W.[2] Alternatively, 22 nm polystyrene beads have been recently trapped in a specially fabricated interferometric cavity that enhances the local electromagnetic field to improve confinement of the particle in the trapping plane at relatively low beam powers.[3] However, such an approach is not easily adaptable to the assembly of truly 3D free-standing nanostructures. In contrast, the approach demonstrated as part of this work uses closed-loop control to both improve the lifetime of nanoparticles in an optical trap and minimize the average laser power input to the system, without requiring any special modifications to the assembly cell.

High-speed closed-loop control using fast photodetectors to measure the particle position in the trap is commonly applied to improve the localization of microscale particles in optical traps. Two methods of control are commonly used: (i) position control, where the trap position is modified in response to particle position, and (ii) intensity control, where the intensity

Received: January 24, 2012
Revised: April 2, 2012
Published: April 10, 2012

   dx.doi.org/10.1021/nl300301x | *Nano Lett.* 2012, 12, 2347–2351

of the trap is modulated as a function of the particle position. Closed-loop controllers are particularly important in biophysics applications, where they have been used to create force and position clamps that enable nanomechanical studies of macromolecules. For example, position control has been essential in understanding the chemomechanical behavior of motor proteins using a force clamp,[4] and intensity control has been used to measure the stiffness of DNA with a position clamp.[5] More recently, position control has been used to suppress the Brownian motion of micrometer-sized particles, improving the localization of these particle within the trap.[6,7] However, existing controllers have not yet been shown to improve the mean lifetime of nanoscale particles in optical traps, as demonstrated below.

A closed-loop controller can modify the position and/or the intensity of an optical trap in response to the movement of the nanoparticle. Therefore, the controller transfer function can generate two control signals as a function of particle position: (i) a vector function describing the target position of the trap and (ii) a scalar function that sets the target intensity of the trap. Control algorithms can be realized in several ways by combining these parameters, depending on the performance objectives and constraints on the system. The main control scheme used in this work is blanking control, a type of intensity control designed to reduce the power of the trapping beam when the particle is close to the trap center. An optical trap, such as the one used in our experiment, has a beam intensity profile that is maximum at the center and decreases away from the origin. However the optical trapping force is zero at the center of the trap.[8] Therefore by blanking the beam close to the center of the trap, we are able to reduce the average power incident on the particle and the surrounding fluid without significantly reducing the trapping force.

We ignore the asymmetry of the optical trap due to laser polarization and design the controller using radial coordinates in the transverse plane. The particle position ($r = (x^2 + y^2)^{1/2}$), in two-dimensional (2D) Cartesian coordinates, is measured relative to the controller set point, which is fixed in the laboratory frame. The controller is designed to set the trap power to its minimum value P_{min} when the particle is inside a blanking region, between the center of the trap and r_b. When the particle leaves this blanking region, the controller increases the beam power linearly, approaching a maximum power P_{max} at the end of a transition region defined by r_b'. Finally, the range over which the controller can operate is defined by the limits of the laser-based detection system, r_d. The control law for blanking control is represented formally using the piecewise function shown in eq 1:

$$P_{xy}(r) = \begin{cases} P_{min} & r < r_b \\ P_{min} + \left(\dfrac{P_{max} - P_{min}}{r_b' - r_b}\right) \times (r - r_b) & r_b \le r < r_b' \\ P_{max} & r \ge r_b' \\ P_{min} & r > r_d \end{cases} \quad (1)$$

As we show later, a controller that reacts only to the radial coordinate of the particle position does not significantly improve trapping lifetime, due to the preferential longitudinal escape of particles. We can eliminate this escape route by modifying the blanking controller to include proportional intensity control that reacts to the absolute Z-position ($|z|$) of the particle as shown in eq 2, where κ_p is the proportional gain of the controller. The final control signal is then calculated by selecting the largest beam power between the XY, and Z controllers, shown in eq 3:

$$P_z(z) = \kappa_p|z| \quad (2)$$

$$P(r, z) = \max(P_{xy}, P_z) \quad (3)$$

We implemented the 3D blanking controller in the laboratory using a field programmable gate array[9] with two 12-bit, 64 MHz A/D converters and four 14-bit, 128 MHz D/A converters (Universal Software Radio Peripheral, Ettus Research).[10] Under controlled trapping, the lifetime of the particles is significantly enhanced. In fact, at equivalent average beam power, the controller is consistently able to trap nanoparticles, under conditions where a corresponding static trap was unable.

Controller performance was experimentally verified using a single beam gradient force optical tweezers instrument. Two separate lasers are used in the experiment; a diode pumped Nd:YAG laser with a wavelength of 1064 nm and 5 W maximum power (J20I-8S-12K/BL-106C, Spectra Physics) is used for trapping and manipulating nanoparticles, while a diode laser with a wavelength of 640 nm (iFLEX-2000, Point Source) is used for fast back focal plane detection of the particle position.[11−13] The trapping laser passes through an electro optic modulator (EOM) (350-80LA/Driver 302RM, Con-Optics Inc.), with a bandwidth that exceeds 200 kHz that is used to control the intensity of the beam. The trapping and detection beams are combined before they are introduced into the microscope objective (CFI Plan Apochromat VC Series 60X/1.20NA water immersion, Nikon). After passing through the specimen plane, the detection beam is separated from the trapping beam and split again by a nonpolarizing cube beam splitter. One arm of the detection beam is imaged onto a quadrant photodiode (QPD), which senses the lateral motion of the trapped nanoparticle (QPD-2901, New Focus). The second beam is imaged onto a photodiode (PD-2032, New Focus) to measure the axial displacement of the particle.

We demonstrate blanking control with 100 nm gold nanoparticles, suspended in deionized water (Ted Pella, P/N: 15711-20). A sample cell, approximately 100 μm thick, was prepared using a microscope slide and cover glass and sealed on all sides using double-sided adhesive tape. We calibrate the detection system to convert the measured particle position in volts to units of length using a 100 nm gold nanoparticle immobilized in gelatin. After locating a single immobilized particle, we raster scan it across the beam focus in three-dimensions using calibrated nanopositioning stages (P-721.SL2, P-733.2CL, Physik Instrumente). The mapping between the physical location of the nanopositioning stages and the response, in volts, of the quadrant photodiode (QPD-2901, New Focus) to lateral movement and the photodiode (PD-2032, New Focus) to axial movements of the particle yields the 3D calibration function for particle position in μm, $\vec{\Phi}(\vec{v}) = \{\hat{x}10v_x, \hat{y}10v_y, \hat{z}(27.9v_z + 47.7v_z^2)\}$, assuming no coupling between the axes. This function is valid over a range of ± 1 μm along the X and Y-axes and -1 μm to $+2$ μm along the Z-axis.

The blanking controller is parametrized using laboratory measurements. The blanking region (r_b) in eq 1 is set close to the maximum force point of the trap to maximize the restoring force acting on the particle.[8] We tune the blanking region to r_b

dx.doi.org/10.1021/nl300301x | Nano Lett. 2012, 12, 2347−2351

= 50 nm with no additional transition region (r_b'). The controller increases the beam power from 0 mW (P_{min}) inside the blanking region to 250 mW (P_{max}) outside. Finally, we set the gain for the *Z*-intensity controller to 550 mW/μm so that the *Z*-intensity controller saturates 450 nm from the trap center.

Figure 1 shows the effect of particle position on the instantaneous trap power for the control parameters defined above. The traces for particle position and beam power have been further filtered using a 20 Hz low pass filter. When the radial position of the particle falls outside the blanking region, the instantaneous beam power is set by eq 1 (black dashed box). On the other hand, inside the blanking region, the beam power is set by the absolute *z*-position of the particle, governed by eq 2 (gray dashed box). Finally, we note that the beam power is high only for very short periods of time, resulting in a low average beam power. Furthermore, as discussed below, the average power on the particle in this setup is significantly lower than the beam power and depends on the position of the particle in the trap.

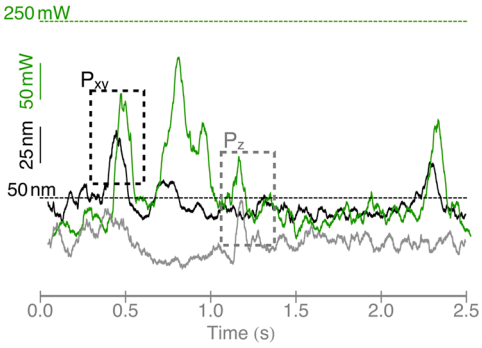

Figure 1. Transverse radial particle position (r) (black), absolute axial displacement (|z|) (gray), and instantaneous beam power (green) as a function of time. For transverse particle movement, the *XY*-controller turns off the beam inside the blanking region (r_b = 50 nm, black, dashed) and the final beam power is set by the *Z*-controller. Outside this region, the *XY*-controller significantly increases the beam power (P_{max} = 250 mW, green, dashed). The dashed boxes show two instances where the radial particle position (black) and axial position (gray) determine the final beam power.

With the control parameters described above, the intensity controller significantly improves the lifetime of a 100 nm gold nanoparticle in the trap. This is clearly seen in Figure 2A,B, which shows a contour plot of the particle positions in the trap in the *XZ*-plane when the controller is off and when it is on. Due to the symmetry of the trap, particle behavior in the *YZ*-plane is not shown.

The contour plots for the 100 nm gold nanoparticles (Figure 2A,B) are generated using the position trajectories of 25 particles, each containing 5 s of data recorded at 20 kHz. For a static trap with average beam power (over time), <*P*> = 60 mW (Figure 2A), the particles are well confined along the transverse axis, while escaping the trap predominantly in the longitudinal direction. This is supported by the nonzero particle density in Figure 2A, well past *Z* = +500 nm until the detector response decreases past 1500 nm, and we are unable to measure the particle position. However, when the controller is on, the behavior is qualitatively different, as seen in Figure 2B. The particles are more strongly localized close to the center of the trap, with no observed escape events over the duration of the experiment. We measure the full width at half-maximum (FWHM) of the particle position distribution along the *X*-axis to be 106 nm, consistent with the controller blanking region (r_b). Particle confinement is excellent longitudinally as well, with no observed density outside of *Z* = ± 600 nm, in contrast with the static trap. Finally, the controller attains this increased localization with the same average beam power (<*P* > = 60 mW) as the static trap.

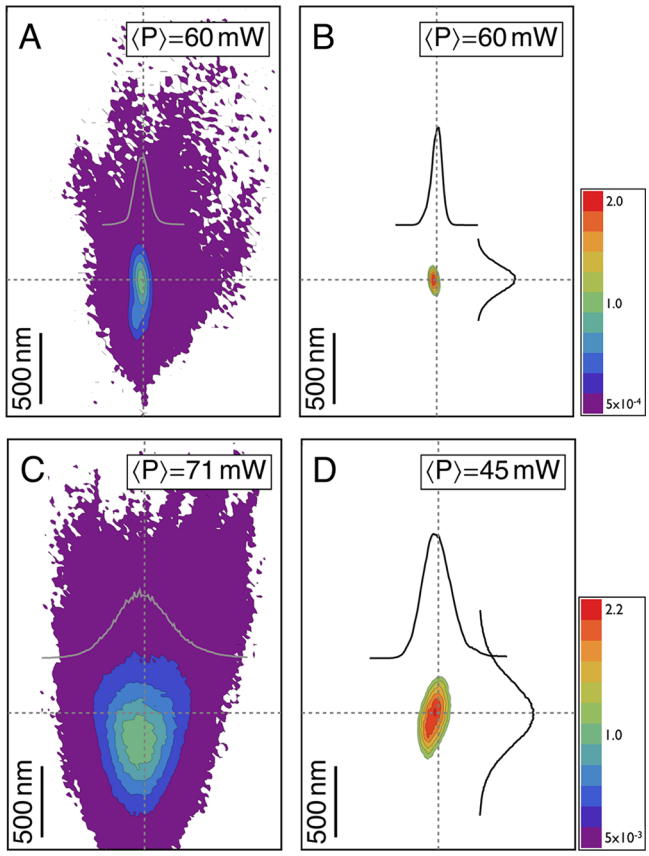

Figure 2. Contour plots of a static optical trap vs controlled trapping, scaled by the maximum counts of the static trap, for 100 nm gold nanoparticles (top) and 350 nm silica particles (bottom) in the *XZ*-plane. The contour lines are evenly spaced. (A) static trap: weakly bound 100 nm gold particles exit the trap very quickly along the longitudinal direction. A histogram of the transverse particle positions through the origin (offset for clarity) is shown. (B) *XYZ* blanking controller: 100 nm gold particles are strongly confined to the trap. The average incident trap power is unchanged from the static trap case. Transverse and longitudinal particle histograms show the particle distributions through the trap center. (C) Static trap: 350 nm silica particles escape the trap predominantly in the longitudinal direction. (D) *XYZ* control: 350 nm silica particles are confined to the trap using one-third less power than the static trap case.

Note that even though the average beam power is the same with the controller on and off, heating may still be reduced. Optical heating may occur due to absorption by the fluid and/or the nanoparticle. In contrast with the intensity of light acting on the fluid, the intensity on a nanoparticle varies with its position in the trap and is calculated by integrating the distribution of particle positions in the trap weighted by the beam intensity. Due to beam blanking, the particle never experiences the most intense part of the beam and therefore sees an even greater decrease in absorbed power during controlled trapping. We estimate the average power incident on

dx.doi.org/10.1021/nl300301x | *Nano Lett.* 2012, 12, 2347−2351

the particle using a Gaussian intensity function that closely approximates generalized Lorentz Mie theory (GLMT) force calculation, described later.[14,15] Under this approximation, the average power incident on the particle for a static trap is estimated to be 3.1 mW. However for the *XYZ* intensity controller, this value is found to be only 0.7 mW or 23% of the static trap case with equivalent beam power.

For the static trap, we estimate the particle's lifetime to be approximately 1.6 s. In comparison, when the controller is on, we observe that no particles exit the trap, and therefore, we are unable to calculate a lifetime. However, by assuming that observed escape events follow a Poisson distribution, we can estimate a lower limit on the lifetime of the particle with 95% confidence to be approximately 42 s, which is significantly greater than the static trap value.[16,10] Finally, we believe the algorithms outlined here leave ample room to optimize multiple performance metrics, including localization.

We have also implemented blanking control with 350 nm diameter silica particles (Bangs Laboratories, P/N: SS02N) to test the effectiveness of this technique with particles of different materials. We also use this result to compare against simulations, performed under equivalent conditions, to better understand the controller behavior. The controller is parametrized by setting the blanking region (r_b) to 125 nm after measuring the entire trapping force profile of the optical trap as a function of distance from the trap center.[8] We set an additional transition region of 10 nm for optimal performance and scale the trap power from 0 mW inside the blanking region to 100 mW outside. Finally, we tune the gain of the *Z*-intensity controller κ_p = 70 mW/μm, so that it attains its maximum power when the particle is 1.4 μm from the center of the trap.

As before, the mean lifetime of the 350 nm glass particles is significantly improved under blanking control, increasing approximately 22-fold over that of a static trap, while using approximately one-third less power ($<P>$ = 45 mW with the controller on, in comparison with $<P>$ = 71 mW for the static trap). This is clearly seen from the contour plots in Figure 2C, where particles escape the trap along the *Z*-axis in the static trap case, characterized by significant particle density well past +1000 nm. On the other hand, Figure 2D shows that the particles remain localized close to the center of the trap, with no observed escape events during these measurements. Finally, under blanking control, the FWHM of the particle position distribution along the transverse axis is estimated to be 277 nm, which is consistent with the size of the blanking region.

We use Langevin dynamics simulations to guide the design of the feedback controllers described above.[17] In fact, simulations were performed earlier than experiments and highlight the importance of including the axial particle position in the control law. We include the optical trapping force in the simulations by implementing a GLMT force calculation.[14,15] This method treats both the gradient and scattering components of the trapping force, acting on arbitrarily sized spherical particles of different materials. We do not include effects of beam truncation or high numerical aperture,[18] as the goal is to estimate relative enhancements in trapping performance from prototype control systems.

The trapping force field used in the simulations is calculated for 350 nm silica nanoparticles, and the wavelength of the incident beam is 1064 nm with a spot size of 550 nm. The refractive index of the particle is assumed to be 1.57 and that of the surrounding water is 1.33. We perform static trap simulations with a constant power of 5 mW as our baseline for these results.

We use two representative controllers in simulations to illustrate the control action. The first simulated controller uses only the transverse particle position to determine the incident beam power. This controller is compatible with detection hardware commonly found in optical trapping instruments, which use back focal plane detection to measure the particle position in the transverse plane but not along the longitudinal axis.[13] Sensitive only to transverse particle excursions, it modifies trap characteristics without enhancing lifetime as seen below.

For the *XY* blanking controller, we set the blanking region, r_b = 275 nm to coincide with the maximum force point predicted by the GLMT model in the transverse *XY*-plane. The controller increases the power rapidly to a maximum value, P_{max} = 25 mW, and exerts a maximum force on the particle when it leaves the blanking region. We set the power inside the blanking region to P_{min} = 0, so that the trap is completely off. We limit the maximum power available to the controller to 25 mW or five times the power used in the baseline static trap simulations.

Figure 3A shows the trajectories in the *XZ*-plane from 100 simulation runs, each 5 s long, using the transverse blanking

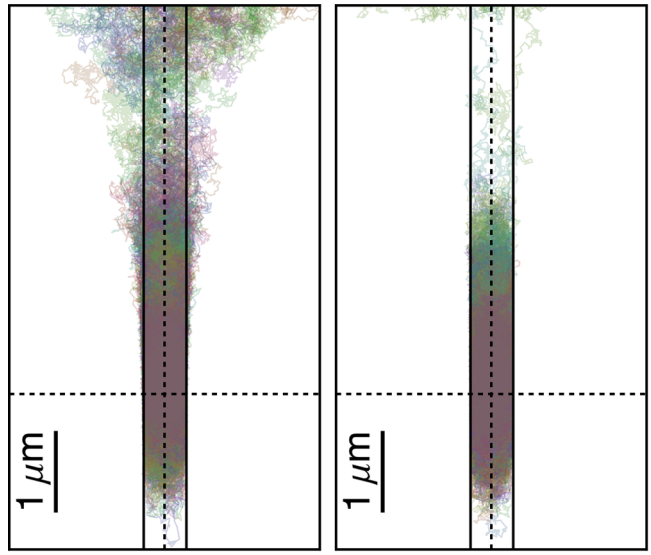

Figure 3. Simulated trajectories for 100 noninteracting 350 nm silica nanoparticles in the *XZ*-plane. (A) *XY* blanking control: The particles are well confined in the transverse direction but escape preferentially along the longitudinal direction due to the scattering force and because the controller does not respond to the longitudinal movement of the particle. (B) *XYZ* blanking control: We observe qualitatively different behavior than the *XY* blanking controller case, highlighting the importance of control action along the longitudinal direction.

controller. Since the trap is circularly symmetric in the transverse plane about the origin, we do not show the *YZ*-plane in the figure. The two solid lines in the plot represent the blanking region. When the particle is within this region, the trap is turned off, and the particle undergoes free diffusion. When the particle crosses the boundary of the blanking region in the transverse direction, the controller increases the trap power to P_{max}, and the particle experiences a restoring force toward the center of the trap. As seen from the plot, the particle diffuses freely to fill up the volume of the blanking region. However the combination of the longitudinal scattering force and the fact

dx.doi.org/10.1021/nl300301x | *Nano Lett.* 2012, 12, 2347−2351

that the controller does not react to the Z-position of the particle results in a preferential escape route for the particle along the positive Z-axis, which causes the particle to quickly exit the trap as seen in Figure 3A.

We quantify controller performance by calculating the mean lifetime of nanoparticles in the trap[10] as well as the average incident power. When using this algorithm, we see no appreciable gain in lifetime, (1.7 ± 0.4) s with the controller on compared with (1.8 ± 0.3) s for the static trap. However, the controller limits the average power to only 5.4 mW, which is consistent with the static trap power (5 mW) despite the fact that the maximum power is five times higher. This is directly a result of the blanking region near the trap center, which greatly reduces the average power used by the controller. However limiting the controller to only the X and Y particle positions leaves an escape route along the Z-axis.

This preferential escape route can be eliminated by extending controller action to react to particle motion in the longitudinal direction using eq 2. The Z-controller gain, κ_p is tuned to 100 mW/μm, so that the controller saturates at $z = \pm 2$ μm with a maximum power, P_{max} = 200 mW. The final control then signal is determined by eq 3. The trajectories for 100 simulated particles in the XZ plane are shown in Figure 3B. From the trajectories in the figure, it is evident that the controller exhibits qualitatively different behavior in comparison with the previous case. Only two particles from the ensemble escape the trap, while most particles are contained within ±275 nm along the X and Y-axes and within ±2 μm along the Z-axis. Moreover since only two particles escape the trap, we are unable to calculate a lifetime but can estimate the lower limit on the lifetime of the particle with 95% confidence to be approximately 80 s, which is significantly greater than the static trap value. We note that even though the controller has an upper power limit of 200 mW (40 times the static trap power), the average power varies between only 4% and 24% higher than the static trap value. Finally, we observe that the improved lifetime obtained using this controller depends heavily on the addition of Z-axis control.

The 20-fold increase in optical trapping lifetime reported here for these proof-of-principle controlled trapping systems leave much potential for improvement. Trap performance (in terms of longer trapping, more localized trapping, or reduced heating) can be enhanced for smaller particles, which advances the prospect not only of nanomanipulation of the smallest particles using optical tweezers but also at reduced power to maintain compatibility with biological systems.

AUTHOR INFORMATION

Corresponding Author

*E-mail: arvind@nist.gov; lebrun@nist.gov.

Notes

The authors declare no competing financial interest.

REFERENCES

(1) Hansen, P. M.; Bhatia, V. K.; Harrit, N.; Oddershede, L. B. *Nano Lett.* **2005**, *5*, 1937−1942.
(2) Seol, Y.; Carpenter, A. E.; Perkins, T. T. *Opt. Lett.* **2006**, *31*, 2429−2431.
(3) Chen, C.; Juan, M. L.; Li, Y.; Maes, G.; Borghs, G.; Van Dorpe, P.; Quidant, R. *Nano Lett.* **2012**, *12* (1), 125−132.
(4) Visscher, K.; Schnitzer, M. J.; Block, S. M. *Nature* **1999**, *400*, 184−189.
(5) Wang, M.; Yin, H.; Landick, R.; Gelles, J.; Block, S. *Biophys. J.* **1997**, *72*, 1335−1346.
(6) Wallin, A. E.; Ojala, H.; Hæggström, E. H.; Tuma, R. *Appl. Phys. Lett.* **2008**, *92*, 224104.
(7) Gorman, J. J.; Balijepalli, A.; LeBrun, T. W. In *Feedback Control of MEMS to Atoms*; Gorman, J. J., Shapiro, B., Eds.; Springer: New York, 2011; pp 141−177.
(8) Balijepalli, A.; Lebrun, T.; Gorman, J.; Gupta, S. "Evaluation of a Trapping Potential Measurement Technique for Optical Tweezers using Simulations and Experiments", Proceedings of the ASME Design Engineering Technical Conferences and Computers and Information in Engineering Conference 2009, San Diego, California, August 30−September 2, 2009; ASME: New York, 2009.
(9) Certain commercial entities, equipment, or materials may be identified in this document in order to describe an experimental procedure or concept adequately. Such identification is not intended to imply recommendation or endorsement by the National Institute of Standards and Technology nor is it intended to imply that the entities, materials, or equipment are necessarily the best available for the purpose.
(10) Balijepalli, A. Modeling and Experimental Techniques to Demonstrate Nanomanipulation with Optical Tweezers. *Ph. D. Thesis*, University of Maryland, College Park, MD, 2011.
(11) Fallman, E.; Axner, O. *Appl. Opt.* **1997**, *36*, 2107−2113.
(12) Balijepalli, A.; Lebrun, T.; Gorman, J.; Gupta, S. "Methods to directly measure the trapping potential in optical tweezers", *Proc. SPIE* **2008**, *70380V*.
(13) Lang, M.; Asbury, C.; Shaevitz, J.; Block, S. *Biophys. J.* **2002**, *83*, 491−501.
(14) Gouesbet, G.; Maheu, B.; Grehan, G. *J. Opt. Soc. Am. A* **1988**, *5*, 1427−1443.
(15) Nahmias, Y.; Odde, D. *IEEE J. Quantum Electron.* **2002**, *38*, 131−141.
(16) Barnett, R.; Carone, C.; Groom, D.; Trippe, T.; Wohl, C.; Armstrong, B.; Gee, P.; Wagman, G.; James, F.; Mangano, M.; Monig, K.; Montanet, L.; Feng, J.; Murayama, H.; Hernandez, J. et al. *Phys Rev D* 1996, *54*, 1−708.
(17) Balijepalli, A.; Lebrun, T.; Gupta, S. *J. Comput. Inf. Sci. Eng.* **2010**, *10*, 011010.
(18) Lock, J. A. *Appl. Opt.* **2004**, *43*, 2545−2554.